Jpn. J. Infect. Dis., 69, 293–299, 2016

Original Article

Measles and Rubella: Scale Free Distribution of Local Infection Clusters

Hiroshi Yoshikura[1]* and Fumihiko Takeuchi[2]

[1]*National Institute of Infectious Diseases, Tokyo 162-8640; and* [2]*Gene Diagnostics and Therapeutics, Research Institute National Center for Global Health and Medicine, Tokyo 162-8655, Japan*

SUMMARY: This study examined the size distribution of local infection clusters (referred to as clusters hereafter) of measles and rubella from 2008–2013 in Japan. When the logarithm of the cluster sizes were plotted on the x-axis and the logarithm of their frequencies were plotted on the y-axis, the plots fell on a rightward descending straight line. The size distribution was observed to follow a power law. As the size distribution of the clusters could be equated with that of local secondary infections initiated by 1 patient, the size distribution of the clusters, in fact, represented the effective reproduction numbers at the local level. As the power law distribution has no typical sizes, it was suggested that measles or rubella epidemics in Japan had no typical reproduction number. Higher the population size and higher the total number of patients, flatter was the slope of the plots, thus larger was the proportion of larger clusters. An epidemic of measles or rubella in Japan could be represented more appropriately by the cluster size frequency distribution rather than by the reproduction number.

INTRODUCTION

Measles is a leading cause of deaths among young children globally, and rubella causes congenital rubella syndrome in mothers infected within 20 weeks of gestation. Both the infections cause rash and fever, and are seasonal and transmitted through respiratory droplets from person-to-person. The World Health Organization launched a measles and rubella elimination program (1). Although the program has progressed, there have been difficulties even in countries that have successfully eradicated polio in the past (2). Why is eliminating measles so difficult?

The elimination of measles requires maintaining the effective reproduction number R to <1 (3), where R is the average number of secondary infections produced when 1 infected individual is introduced into a host population where everyone is susceptible (4). However, the size distribution of the secondary infections, which is crucially important for interpreting the average, has rarely been examined directly during actual epidemics. This study examined the frequency distribution of the sizes of local infection clusters of measles and rubella in Japan from 2008–2013.

MATERIALS AND METHODS

As per the Infectious Disease Control Law in Japan, since 2008, it is obligatory for physicians to notify within 7 days all the cases of measles and rubella diagnosed by them (5). The weekly incidence of measles and rubella in each prefecture has been monitored by the National Epidemiological Surveillance of Infectious Diseases (NESID) (6–7). As there are 47 prefectures in Japan and 1 year consists of 52 weeks, the data could be presented as a 47 × 52 lattice as shown in Table 1. In this study, a cluster is defined as a group of patients reported from the same prefecture in successive weeks, with at least 1 week of 0 reporting before and after a certain instance of reporting. For example, if the numbers of patients reported weekly by a prefecture appears in the order of 0-0-1-0-2-3-1-0⋯, the underlined groups of figures "1" and "2-3-1" would each constitute a cluster. A cluster has 2 parameters of size, the total number of patients (mass) and the duration of uninterrupted measles reporting (length). Thus, cluster "1" has a mass of 1 and length of 1, and cluster "2-3-1" has a mass of 6 and length of 3. To determine the mass and length, clusters were grouped in size ranges, such as 2^0, 2^1, $>2^1$–2^2, $>2^2$–2^3⋯, and the upper limit of the size range was used to represent the size of each group. The frequency of the size was calculated by adding the numbers of clusters within the size range. For example, a cluster of size 2^3 consists of clusters of sizes 5, 6, 7, and 8. If the frequencies of the respective sizes are 1, 0, 2, and 0, the frequency of the cluster is calculated as $1 + 0 + 2 + 0 = 3$.

A cluster could be produced by a local virus spread or by chance. Therefore, we examined whether the obtained cluster size distribution could be explained by the chance event or not. Fig. 1A shows a simulation of chance events obtained by tossing 125, 250, 500, 1,000, 2,000, 4,000, 8,000, or 16,000 coins into a 47 × 52 lattice at random, and estimating the frequency distribution of the mass sizes of the clusters as defined above. The horizontal axis indicates the cluster mass size and the vertical axis denotes its frequency. When 125, 250, or 500 coins were tossed, the plots approximately fell on straight lines; the slopes -s, the coefficient of x, obtained by the logarithmic approximations were -2.578, -1.808, and -1.377, respectively. When 500 or more coins were tossed, the plots became convex and when the number of coins reached 16,000, the plots further departed from the straight line (panel A). The same data

Received June 25, 2015. Accepted September 17, 2015.
J-STAGE Advance Publication November 13, 2015.
DOI: 10.7883/yoken.JJID.2015.308
*Corresponding author: Mailing address: Department of Food Safety, Ministry of Health Labour and Welfare, 1-2-2 Kasumigaseki, Chiyoda-ku, Tokyo 100-8916, Japan.
E-mail: yoshikura-hiroshi@mhlw.go.jp

Table 1. Table for counting infectious clusters of different sizes (measles 2010) -an example

Prefecture	Population*	Week																																																			
		1	2	3	4	5	6	7	8	9	10	11	12	13	14	15	16	17	18	19	20	21	22	23	24	25	26	27	28	29	30	31	32	33	34	35	36	37	38	39	40	41	42	43	44	45	46	47	48	49	50	51	52
Tottori	578																																																				
Shimane	702																																																				
Kochi	745																																																				
Tokushima	770																																																				
Fukui	795																																																				
Saga	840																																																					
Yamanashi	847				2													1																																		1	
Kagawa	979																																																				
Wakayama	985																																																				
Akita	1,050																											1																									
Toyama	1,076											1																																									
Miyazaki	1,120																																			1	2	3	1	1													
Yamagata	1,141																																																				
Ishikawa	1,159																																																				
Oita	1,178																																																				
Iwate	1,295									1	1																																										
Aomori	1,335																																																				
Okinawa	1,383																																																				
Nara	1,397																																																				
Shiga	1,405				1																																																
Nagasaki	1,415																							1																													
Ehime	1,416																									1													1														
Yamaguchi	1,420																																																				
Kagoshima	1,680																						1																														
Kumamoto	1,801																																																				
Mie	1,833																																		1																		
Okayama	1,930			2			2	1																	1																												
Tochigi	1,946						1		3		1						1			1					1			2																									
Gunma	1,984																																																				
Fukushima	1,986																					1	2		2						2																						
Gifu	2,051				1	3									1																									1													
Nagano	2,122																																																				
Miyagi	2,328																																																				
Niigata	2,330												1							1																																	
Kyoto	2,617																								1															1													
Hiroshima	2,840	1										1											1								1					2																	
Ibaraki	2,931																																																				
Shizuoka	3,723						1																		1																												
Fukuoka	5,090																																																				
Hokkaido	5,431																													1																							
Hyogo	5,558												1	1		1		1			1	1	1	2		1	1	1						1	2						1												
Chiba	6,192	1			3		3	1	1			1			1						1				1				1			1		1		1	1	1							1	1		1			1		
Saitama	7,222								1	1	1			1		1	1		1	1	1	3	1	1	1	2		2			2	1	2		1	1								1				1					
Aichi	7,443	3	1	1		5	3	4	3		4	3	1	1		1								2				1		1			1			1					1		1					1					
Osaka	8,849						1							1									1			1																											
Kanagawa	9,079			1	1			1					2			1			1							1	1	1	3		1	1	1			1	3		1							1				1		1	
Tokyo	13,300	1	3			1	3	1	1	1	1	1	2	2							2		1	1	3	4	2	4	4	5	5	5	1	3	3	5	1	1	1	1	2	1	1				2	2	3	2	2		1

* ×1,000.

Vacant boxes indicate 0 incidences

Row: prefectures; colum: weeks of a year starting from the 1st week of January. Thirteen prefectures with polulation ≥2,617 × 1,000 are shaded.

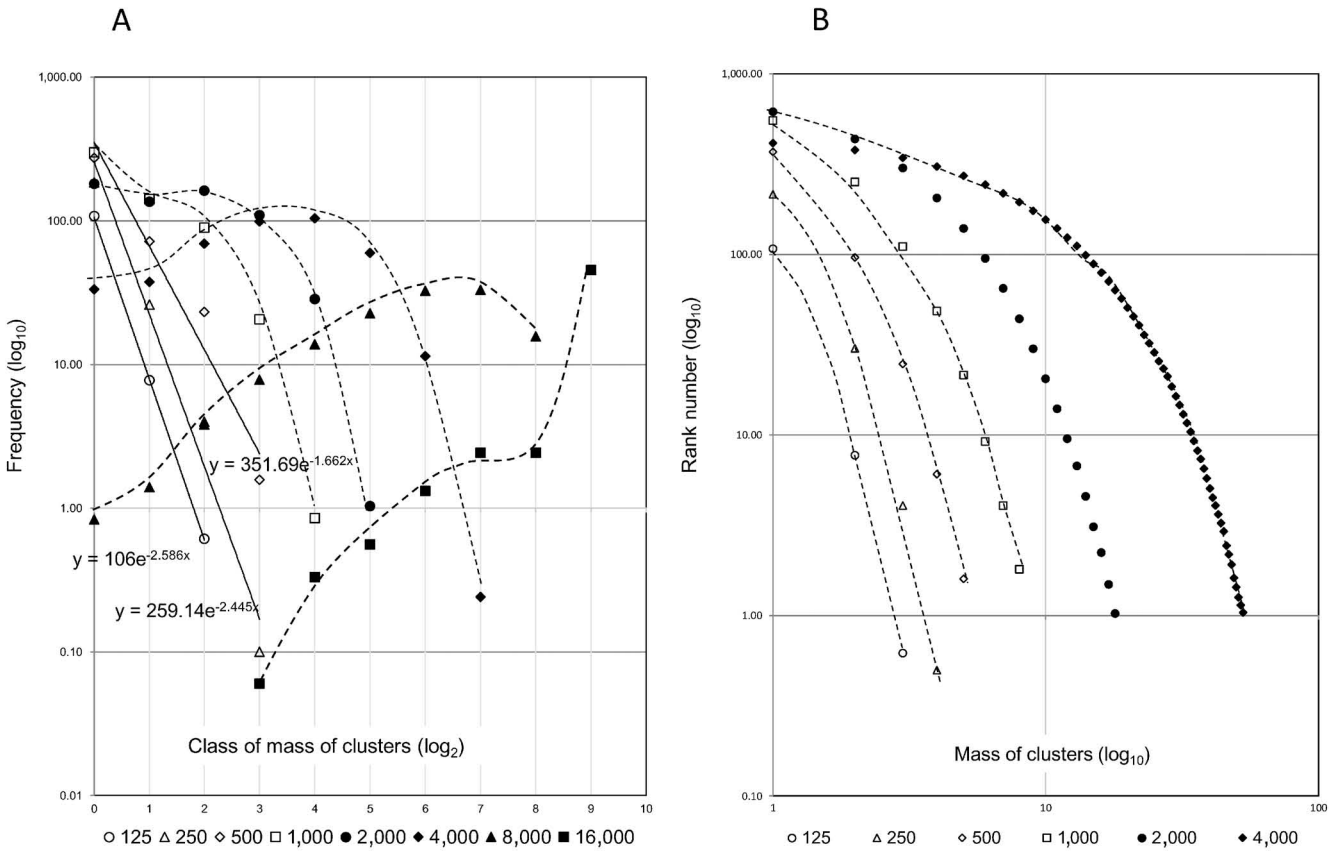

Fig. 1. Expected variations of mass sizes of clusters for different annual patient numbers. Panel A: simulated frequency distribution of classes of mass of local infection clusters. Horizontal axis: classes of mass of clusters (in $\log_2$); vertical axis: their frequencies (in $\log_{10}$). The approximations for coin numbers 125, 250, and 500 were $y = 106e^{-2.586x}$, $y = 259.14e^{-2.445x}$, and $y = 351.69e^{-1.662}$, which were inserted for comparison to the actual data with the simulation assuming occurrence at random. Panel B: Zipf plot to the simulated data. Horizontal axis: mass of clusters (in $\log_{10}$); vertical axis: rank number (in $\log_{10}$).

were used for the Zipf type plots (8), where the clusters were ranked in the descending order of the mass size, and the mass size was plotted on the horizontal axis and the rank on the y-axis in the logarithmic scale (panel B). The plots were generally concave, and did not fall on straight lines (Fig. 1B).

RESULTS

The upper panels of Fig. 2 show the plots of size versus its frequency. All the plots fell on rightward descending straight lines, which could be approximated by the equation $y = Ae^{-sx}$, where x denotes the $\log_2$ of the size, y denotes its frequency, and constants A and -s are the y-intercept (at $x = 2^0$) and the slope, respectively. In the case of the mass of measles (panel A1-M), the approximation straight lines followed equations $y = 67.7e^{-0.38x}$ for 2008 (11,012 patients), $y = 110.1e^{-0.74x}$ for 2009 (732 patients), $y = 93.8e^{-0.89x}$ for 2010 (447 patients), $y = 50.1e^{-0.52x}$ for 2011 (439 patients), $y = 34.2e^{-0.64x}$ for 2012 (283 patients), and $y = 61.2e^{-0.59x}$ for 2013 (229 patients). The slopes -s, $-0.38 \sim -0.89$, for 2009–2013, were flatter than the slopes $-2.586 \sim -1.662$ expected from the random events (the plots for the tossed coins 150–500 in Fig. 1A). The plots for 2008 with 11,012 patients fell on a straight line, with the slope $-s = -0.59$, even though convex curves were expected from the random events (the plots for the tossed coins 8,000 or 16,000 in Fig. 1A). Essentially the same observations were made for the length of measles (panel A1 – L). The Zipf type plots (8), log-log plot of the mass (panel A2-M) or the length (panel A2-L) in the x-axis and the rank number in the y-axis, fell on straight lines even though the random process predicted convex curves. The plots for the mass of rubella (panels B1-M and B2-M) were essentially the same as those for the mass of measles.

Thus, for both measles and rubella, the frequency distributions of local infection cluster sizes could not be explained by chance events. The secondary infections initiated by 1 patient must have been the main cause of formation of the clusters. Because reproduction number was defined as the average number of secondary infections produced by a typical infective person (4), the frequency distribution of cluster sizes was equivalent to the frequency distribution of the reproduction numbers.

Thus, the frequency distribution of the reproduction number of measles and rubella followed a power law (8–15). The mean and variance of power law probability distributions can become infinite when the slope is flat due to frequent large-size events (8). Therefore, applying conventional statistics based on variance and standard deviation can be inappropriate to represent measles or rubella epidemics in Japan.

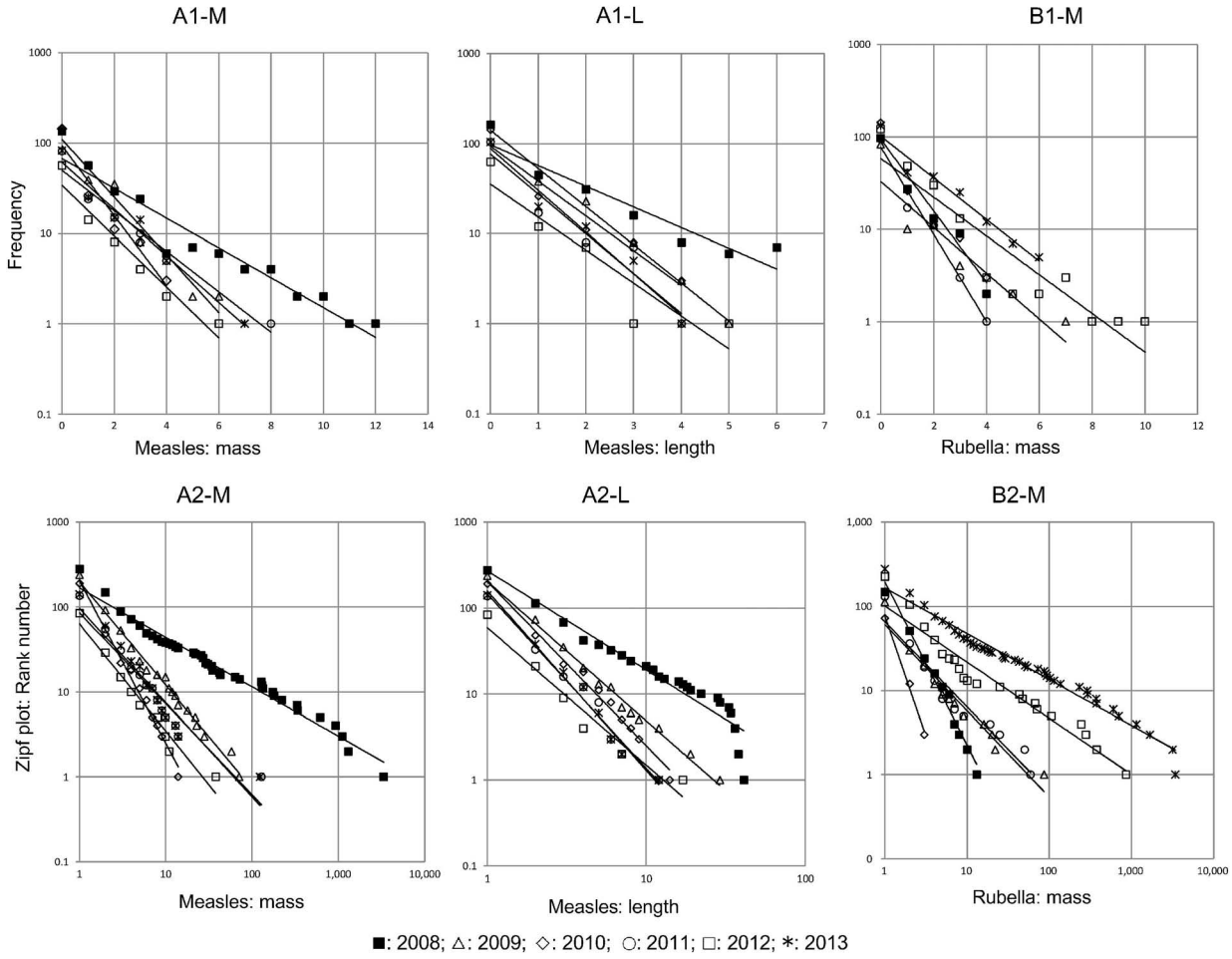

Fig. 2. Frequency distribution of mass and length of measles clusters. ■: 2008; △: 2009; ◇: 2010; ○: 2011; □: 2012, *: 2013. For A1-M, A1-L, and B1-M, x-axis: classes of mass or length; y-axis their frequencies. For A2-M, A2-L, and B2-M, the x-axis indicates mass or length, and the y-axis rank number. Logarithmic approximations for frequency distribution and power approximation for Zipf plot were: A1-M (measles: frequency distribution of classes of ''mass''): 2008: $y = 67.7e^{-0.38x}$; 2009: $y = 110.1e^{-0.74x}$; 2010: $y = 93.8e^{-0.89x}$; 2011: $y = 50.1e^{-0.52x}$; 2012: $y = 34.2e^{-0.64x}$; 2013: $y = 61.2e^{-0.59x}$. A2-M (measles: Zipf plot of ''mass''): 2008: $y = 167.3x^{-0.58}$, 2009: $y = 198.9x^{-1.21}$; 2010: $y = 204.3x^{-1.91}$; 2011: $y = 85.8x^{-1.07}$; 2012: $y = 63.6x^{-1.26}$; 2013: $y = 97.1x^{-1.11}$. A1-L (measles: frequency distribution of classes of ''length''): 2008: $y = 97.3e^{-0.53x}$; 2009: $y = 141.5e^{-0.98x}$; 2010: $y = 93.8e^{-0.89x}$, 2011: $y = 76.8e^{-1.02x}$, 2012: $y = 35.3e^{-0.84x}$, 2013 $y = 88.4e^{-1.07x}$. A2-L (measles: Zipf plot of length): 2008: $y = 271.8x^{-1.15}$; 2009: $y = 204.4x^{-1.62}$; 2010: $y = 204.3x^{-1.91}$; 2011: $y = 147.3x^{-2.03}$; 2012: $y = 59.2x^{-1.60}$; 2013: $y = 159.1x^{-2.09}$. B1-M (rubella: frequency distribution of classes of ''mass''): 2008: $y = 84.6e^{-0.89x}$; 2009: $y = 50.1e^{-0.84x}$; 2010: $y = 52.5e^{-1.50x}$; 2011: $y = 77.1e^{-1.08x}$; 2012: $y = 129.1e^{-0.85x}$; 2013: $y = 101.7e^{-0.52x}$. B2-M (rubella: Zipf plot of ''mass''): 2008: $y = 75.8x^{-2.86}$; 2009: $y = 60.5x^{-1.02}$; 2010: $y = 75.8x^{-2.86}$; 2011: $y = 65.1x^{-1.01}$; 2012: $y = 100.5x^{-0.66}$; 2013 'y = $165.2x^{-0.54}$.

For measles, the slope for 2009–2013 was steeper, with fewer cases (447, 732, 439, 283, and 229 in the respective years), than that for 2008, with a larger number of cases (11,012 cases). For rubella, the slope for 2008–2011 was steeper, with fewer cases (293, 87, 147, and 378 in the respective years), than that for 2012–2013, with more cases (2,386 and 14,433 in the respective years). Thus, higher the total number of patients, flatter was the slope, and lower the total number of patients, steeper was the slope. In other words, higher the total number of patients, higher was the proportion of large-sized clusters, and lower the total number of patients, higher was the proportion of small-sized clusters.

As the epidemics of measles and rubella were under the influence of population size/density (16), the prefectures were divided into 2 groups, a small-sized prefecture group (34 prefectures with a population $\leq$2,330 × 1,000) and a large-sized prefecture group (13 prefectures with a population $\geq$2,617 × 1,000) (Table 1). As shown in Fig. 3, the slope for the mass and length was steeper for the small-sized prefecture group than that for the large-sized prefecture group (panels A1-M and A1-L for the mass and length of measles and panel B1-M for the mass of rubella). In panels A2 and B2 in Fig. 3, the slope -s is plotted against the total number of patients in the 2 prefecture groups. The plots for the large prefecture group were observed to be above those for the small prefecture group and the distribution of the plots showed the right side rising. The data suggested that higher the population size and/or larger the total number of patients, flatter was the slope, and consequently,

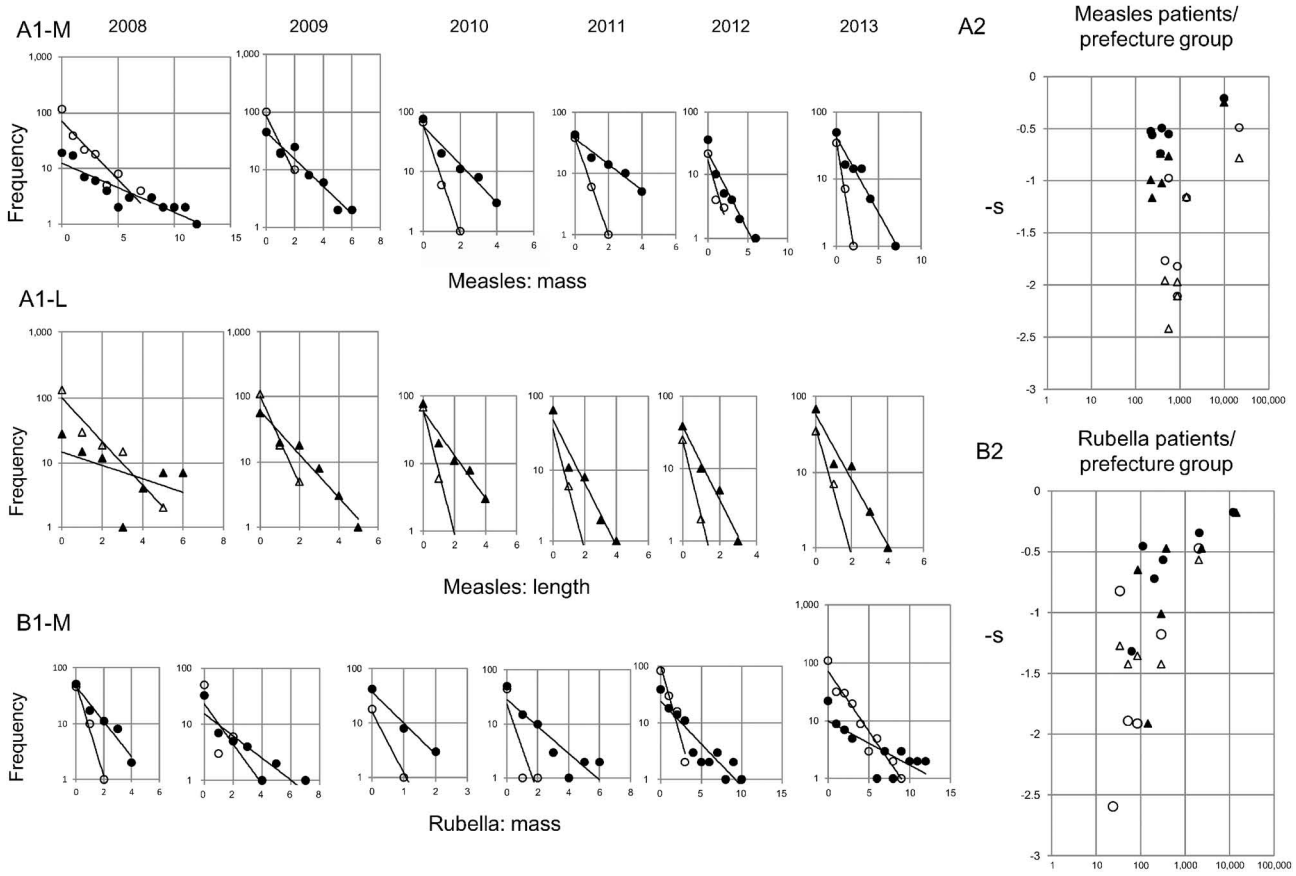

Fig. 3. Frequency distribution of mass and length of clusters. ○: mass of clusters for measles or rubella in small sized prefecture group; ●: mass of clusters for measles or rubella in large-sized prefecture group; △: length of clusters for measles or rubella in small-sized prefecture group; ▲: length of clusters for measles or rubella in large sized prefecture group. The approximations for small sized and large sized prefectures were respectively: A1-M: frequency distribution of classes of mass of measles: $y = 71.6e^{-0.49x}$ and $y = 12.4e^{-0.20x}$ for 2008; $y = 87.3e^{-1.16x}$ and $y = 45.2e^{-0.55x}$ for 2009; $y = 60.4e^{-2.10x}$ and $y = 97.8e^{-0.74x}$ for 2010; $y = 137.7e^{-1.82x}$ and $37.3e^{-0.49x}$ for 2011; $y = 16.7e^{-0.97x}$ and $21.7e^{-0.56x}$ for 2012; and $y = 41.6e^{-0.52x}$ and $y = 36.1e^{-1.76x}$ for 2013; A1-L: frequency distribution of classes of length of measles: $y = 102.1e^{-0.78x}$ and $y = 14.9e^{-0.24x}$ for 2008; $y = 100.0e^{-1.54x}$ and $y = 59.4e^{-0.76x}$ for 2009; $y = 60.4e^{-2.10x}$ and $y = 57.8e^{-0.74x}$ for 2010; $y = 38.0e^{-1.97x}$ and $y = 50.6e^{-1.02x}$ for 2011; $y = 24.1e^{-2.41x}$ and $y = 37.6e^{-1.16x}$ for 2012; and $y = 39.3e^{-1.96x}$ and $y = 57.7e^{-0.99x}$ for 2013; B1-M: frequency distribution of classes of mass of rubella: $y = 52.4e^{-1.9x}$ and $y = 46.2e^{-0.73x}$ for 2008; $y = 23.2e^{-0.83x}$ and $y = 15.5e^{-0.46x}$ for 2009; $y = 16.3e^{-2.60x}$ and $y = 37.5e^{-1.32x}$ for 2010; $y = 23.4e^{-1.89x}$ and $y = 28.3e^{-0.57x}$ for 2011; $y = 98.7e^{-1.18x}$ and $y = 23.8e^{-0.35x}$ for 2012; and $y = 71.5e^{-0.48x}$ and $y = 9.9e^{-0.18}$ for 2013. For any plot, if y was ≥ 1 at $x = 0$ and at $x = 1$ and if y was 0 at $x = 2$, 0.1 was used as the y coordinate at $x = 2$ for graphics convenience. Panels A2 and B2: Plots of total number of patients in the x-axis versus the coefficient of x, -s, in the y-axis. Panel A: measles; panel B: rubella. Each plot represents each year. ○: mass of the small prefecture group; ●: mass of large prefectures; △: length of small prefectures; ▲: length of large prefectures.

the proportion of large-sized clusters increased.

DISCUSSION

The above observations have been summarized in the following paragraphs. First, the distribution of the cluster sizes was scale-free or followed a power law (8–15). The kinetics can be explained using a model depicted in Fig. 4A. If an epidemic starts with N number of infections, at step 1, the fraction p of N, i.e., pN, transmits the infection to the next case to become the seed of further expansion, and (1-p)N remains as size = 2^0 to become the dead end. At step 2, the fraction p of pN, i.e., p^2N, transmits the infection to the next case, and the fraction (1-p) of pN, i.e., (1-p)pN, remains as size = 2^1 to become the dead end. Similarly, at step i, the fraction p of p^{i-1}N, i.e., p^iN, transmits the infection, and the fraction (1-p) of p^{i-1}N, i.e., (1–p) p^{i-1}N, remains as size = 2^{i-1} to become the dead end. Thus, the frequency of sizes 2^0, 2^1, 2^2, 2^3, $2^4 \cdots 2^{i-1}$ will be (1–p)N, (1–p)pN, (1–p)p$^2N \cdots$(1–p)p$^{i-1}N \cdots$, i.e., cluster size variation follows geometric distribution. A simplified model is shown in Fig. 4B, where p = 1/2 and N = 16. The parameter p can be equated to the slope of the plots, which was $e^{-0.52}$ (= 1/1.68 = 0.6), and N to the total number of clusters counted, which was 278. Thus, 101 infections from the initial 278 infections were considered aborted from further expansion. This analysis indicated the epidemiological importance of clusters with only 1 patient. Higher the proportion of isolated cases, higher were the transmission barriers, such as a lower population size/density or higher population immunity. (In this model, the step was considered in terms of steps of local transmissions and not in terms of the

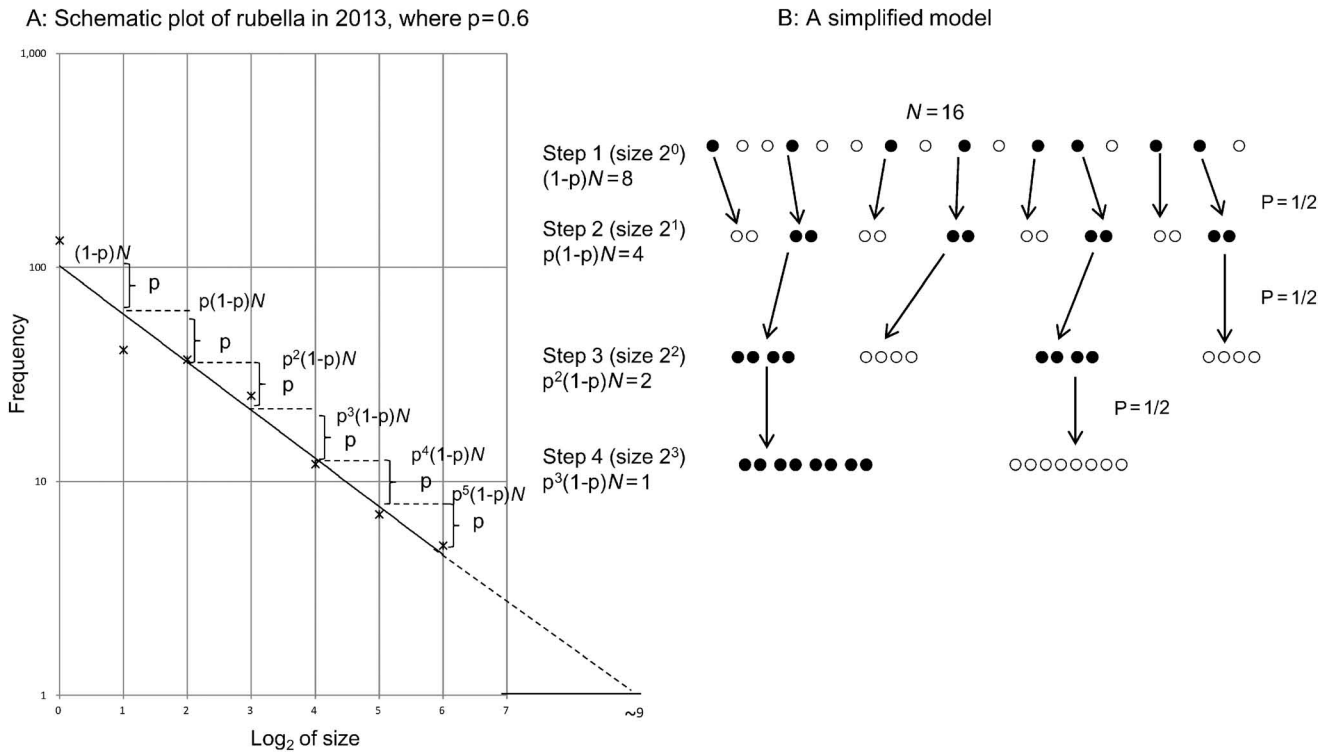

Fig. 4. Model of measles/rubella epidemics. Panel A: schematic presentation of 2013 rubella epidemic. The extrapolation of the plots to the x axis gave $2^{\sim 9} = \sim 500$. Panel B: Simplified model epidemic with p = 1/2 and N = 16. ●: patients that infected others; ○: patients that failed to infect others. See text for further explanation.

real time scale).

The model, though simplistic, is compatible with the findings of the current measles and rubella epidemics in Japan. The transmission will be limited to person-to-person contact during the short period of 4–7 days preceding symptom development because adults, who dominate the patient population (17), will rarely go out with rash and fever. As a measles/rubella epidemic depended not only on demography but also on the ongoing epidemic (Fig. 3 panels A and B), the virus will spread more easily in the area where the virus has spread successfully (as long as sensitive population remains). Fig. 4B shows a simplified presentation of the model with N = 16 and p = 1/2. It was compatible with the virus spread on pre-existent (often unperceived, such as, workplace, schools, etc.) scale-free human networks rather than random spread. The large local infection clusters can be associated with infection of *hubs* (18). Meanwhile, because of high contagiousness, measles and rubella virus will spread to other prefectures to become new seeds. If the virus moves to populated places and finds *hubs*, it will produce large infection clusters, whereas if it strays into less populated places with fewer *hubs*, the secondary spread will be aborted. Compatibility of the above data with the SIR model (4) may require further investigation.

Second, when the prefectures were grouped into those with a large population and those with a small population, the plots for these subgroups fell again on straight lines, i.e., if the parental group followed the power law, the subgroups also followed the power law.

Third, the slope was always flatter for the large prefecture group than that for the small prefecture group, i.e., higher the population size, larger was the proportion of the larger clusters (Fig. 3, panels A1-M, A1-L, and B1-M), consistent with the previous observation that higher the population size/density, higher was the incidence of measles or rubella (16). Panels A2 and B2 in Fig. 3 show that with increase in the number of patients, the slope of the plots became flatter, and with decrease in number of patients, the slope of the plots became steeper. Measles and rubella epidemics seem to be autocatalytic. This property of measles epidemic may explain why measles elimination was accomplished relatively quickly in some regions, but has been difficult in other regions (19).

Fourth, as already indicated, clusters defined in the present analysis could be regarded as local secondary spreads initiated by 1 patient, which were equivalent to secondary infections produced by a typical infective person (reproduction number) (4). Thus, the frequency distribution of the reproduction number, at least in terms of local spread, of measles or rubella in Japan, followed the power law, i.e., it had no typical size. Therefore, the slope -s and the maximum cluster size x_{max} of the scale-free distribution $y = Ae^{-sx}$ were better indicators of an epidemic because the mean and variance of the true distribution can become infinite (8), which depart from the statistics computed from the observed data. The maximum cluster size, x_{max}, can be approximated by the x coordinate for y = 1, i.e., $x_{max} = (\ln A)/s$. For example, in determination of the mass of the rubella epidemic in 2013, the approximations were $y = 101.7e^{-0.52x}$, s = 0.52, and $x_{max} = \ln 101.7/0.52 = 4.62/0.52 = 8.9$, i.e.,

2^9 or about 500 (corresponding with the extrapolation to the x-axis of the plots of rubella in 2013 in Fig. 4A). Another indicator, which is much simpler, would be the proportion of clusters with only 1 patient among the total clusters, i.e., 101 in 278 in the above example.

Lastly, though the cluster size was equal to the size of secondary infection starting from an infective person in the present analysis, ideally, the claim has to be verified by epidemiological and virological investigations of every cluster. However, such a study, if not impossible, is very difficult in practice. For example, in spite of the greatest efforts made by the people involved in measles elimination in Japan in 2014, among the total 1,047 notified cases, only 421 could be laboratory confirmed and only 13 could be linked epidemiologically (20). In addition, the NESID database is currently disconnected from the laboratory database. In the current situation, this problem could be assessed by applying the method to various infections with different transmission modes to evaluate if their frequency distribution is compatible with their transmission modes.

Conflict of interest None to declare.

REFERENCES

1. World Health Organization. Global measles and rubella strategic plan: 2012–2020. Available at <http://www.measlesrubellainitiative.org/wp-content/uploads/2013/06/Measles-Rubella-Strategic-Plan.pdf>. Retrieved in May 2015.
2. Takashima Y, Schluter WW, Mariano KLM, et al. Progress toward measles elimination –Philippines, 1998–2014. MMWR Morb Mortal Wkly Rep. 2015;64:357-62.
3. Gay NJ. Theory of measles elimination: implications for the design of elimination strategies. J Infect Dis. 2004;189:S27-35.
4. Anderson RM, May RM. Infectious Diseases of Humans: Dynamics and Control. Oxford: Oxford University Press; 1991. p. 17-9.
5. Ministry of Health Labour and Welfare. Notification of patients under the Infectious Disease Control Law. Available at <http://www.mhlw.go.jp/stf/seisakunitsuite/bunya/kenkou _ iryou/kenkou/kekkaku-kansenshou/kekkaku-kansenshou11/01.html>. Retrieved in May 2015.
6. National Institute of Infectious Diseases and Tuberculosis and Infectious Diseases Control Divi-sion, Ministry of Health, Labour and Welfare. The National Epidemiological Surveillance of Infectious Diseases in compliance with the enforcement of the new Infectious Diseases Control Law. Infect Agents Surveillance Rep. 1999;20:88'-90'.
7. National Epidemiological Surveillance of Infectious Diseases. Available at <http://www.nih.go.jp/niid/ja/all-surveillance/2270-idwr/nenpou/4317-kako2012.html; http://www.nih.go.jp/niid/ja/survei/2270-idwr/nenpou/5281-syulist2013.html>. Retrieved in May 2015.
8. Newman ME. Power laws, Pareto distribution and Zipf's law. arXiv:cond-mat/0412004v3 [cond-mat.stat-mech] 29 May 2006. Available at <http://arxiv.org/pdf/cond-mat/0412004.pdf>. Retrieved in May 2015.
9. Bak P. How Nature Works–the Science of Self-organized Criticality. New York: Springer-Verlag; 1996. p. 15.
10. Buchanan M. Ubiquity–Why catastrophes happen. New York, NY: Three Rivers Press; 2002. p. 41-62.
11. Johnston AC. Nava S. Recurrence rates and probability estimates for the New Madrid seismic zone. J Geophys Res. 1985;90:6737-53.
12. Mandelbrot B. The variation of certain speculative prices. J Business. 1963;36:394-419.
13. Malamud BD, Morein G, Turcotte DL. Forest fires: an example of self-organized critical behavior. Science. 1998;281:1840-2.
14. Rhodes CJ, Anderson RM. Power laws governing epidemics in isolated populations. Nature. 381;1996:600-2.
15. Trottier H, Philippe PJ. Scaling properties of childhood infectious diseases epidemics before and after mass vaccination in Canada. Theoret Biol. 235;2005:326-37.
16. Yoshikura H. Impact of population size on incidence of rubella and measles in comparison with that of other infectious diseases. Jpn J Infect Dis. 2014;67:447-57.
17. Yoshikura H. Which age group is spreading measles in Japan? Jpn J Infect Dis. 2013;66:459-62.
18. Barbasi AL. Linked–the New Science of Networks. Cambridge, MA: Perseus Publishing; 2002. p. 55-78.
19. Yoshikura H. Population size/density dependency hypothesis for measles epidemic: application of the hypothesis to countries in five WHO regions. Jpn J Infect Dis. 2013;66:165-71.
20. World Health organization Western Pacific Region. Measles Elimination Country Profiles (data through December 2014, as of February 2015), 2015.